AIP | Review of Scientific Instruments

Development and characterization of very dense submillimetric gas jets for laser-plasma interaction

F. Sylla, M. Veltcheva, S. Kahaly, A. Flacco, and V. Malka

Citation: Rev. Sci. Instrum. **83**, 033507 (2012); doi: 10.1063/1.3697859
View online: http://dx.doi.org/10.1063/1.3697859
View Table of Contents: http://rsi.aip.org/resource/1/RSINAK/v83/i3
Published by the American Institute of Physics.

Development and characterization of very dense submillimetric gas jets for laser-plasma interaction

F. Sylla,[1,a)] M. Veltcheva,[1,2] S. Kahaly,[1,b)] A. Flacco,[1] and V. Malka[1]
[1]*Laboratoire d'Optique Appliquée, ENSTA-ParisTech, CNRS, Ecole Polytechnique, UMR 7639, 91761 Palaiseau, France*
[2]*Dipartimento di Fisica "G. Occhialini," Università degli Studi di Milano-Biccoca, piazza della Scienza 3, 20126 Milan, Italy*

(Received 12 October 2011; accepted 5 March 2012; published online 29 March 2012)

We report on the characterization of recently developed submillimetric He gas jets with peak density higher than 10^{21} atoms/cm^3 from cylindrical and slightly conical nozzles of throat diameter of less than 400 μm. Helium gas at pressure 300−400 bar has been developed for this purpose to compensate the nozzle throat diameter reduction that affects the output mass flow rate. The fast-switching electro-valve enables to operate the jet safely for multi-stage vacuum pump assembly. Such gaseous thin targets are particularly suitable for laser-plasma interaction studies in the unexplored near-critical regime. © *2012 American Institute of Physics*. [http://dx.doi.org/10.1063/1.3697859]

I. INTRODUCTION

The use of gas jet targets to generate a suitably dense, reliable, and reproducible interaction medium is particularly important in the broad field of laser-plasma interactions, where they are copiously employed for relativistic laser-plasma interaction for electron acceleration (LPA)[1–5] or ion acceleration,[6,7] parametric instabilities studies,[8–11] atomic physics,[12] investigations of inertial confinement fusion,[13] X-ray lasers,[14] and high harmonic generation.[15]

The control of the gas flow is essential in order to provide the desired interaction density. For example, the use of a sonic or a supersonic gas flow provides a gaussian-like or plateau neutral density profile. By changing the gas pressure, one can change the initial neutral density and by using a combination of gases, one can obtain plasmas with multiple ions species, which is needed to localize electrons injection for innovative laser-plasma accelerator schemes.[16,17] Also, changing the nozzle diameter changes the plasma length, which for LPA schemes allows to control the electron energy and for parametric instabilities studies allows a fine measurement of the corresponding growth rates.

Compared to the thin-foil-explosion techniques, the use of a gas jet presents some interesting advantages. In the previous case, the laser beam impinges on the target, which explodes symmetrically, with a density decreasing rapidly from the solid density to the sub-critical desired density, giving a parabolic longitudinal density profile, for which density and length are interdependent. In contrast, homogeneous plasmas with independent adjustable lengths and density can be produced with pre-ionized gas jets, with a much better reproducibility.[18,19] In addition gas jet targets can be used with a high repetition rate lasers[2] at a reasonable cost and without any requirement for beam realignment and/or mechanical target movement between two consecutive shots.

Up till now, maximum gas densities were limited to about 10^{20} cm^{-3} over few millimeters. For a fully ionized helium gas, the corresponding electron density was therefore limited to twice this value. The critical electronic density n_c of a plasma irradiated by a Ti:Sapphire laser beam of central wavelength $\lambda = 810$ nm is 1.68×10^{21} cm^{-3}, and sets in the non-relativistic case the density limit above which the electromagnetic wave cannot propagate. The maximum electron density was therefore limited to about tens of percent of the critical density, indicating that the range of densities for Ti:Sapphire solid-state lasers that one could explore so far was only underdense. We present in this article a novel apparatus that allows to gain more than a factor of 10 in atomic density, allowing to reach an unexplored range of densities from tens of percent of the critical density to overcritical density and over hundreds of microns only. For this apparatus, we experimented successfully an alternative method of varying the density by probing it during the transient regime, rather than changing the backing pressure. This switches from a pressure to a time adjustment of greater accuracy and ease of implementation.

II. STATEMENT OF THE PROBLEM

Stationary gaseous supersonic jets produced by axisymmetric nozzles have been specifically studied[20] and extensively used[21] over the past decade for laser-plasma interaction experiments. They provide suitable support for plasmas of tunable electronic density n_e, length L, and gradient scale length l (typically $n_e \sim$ few 10^{19} cm^{-3}, $L \sim 1$ mm, and $l \sim 100$s of μm). The tuning is achieved by optimizing the nozzle geometry (throat and exit diameters) and by varying the back pressure feeding the nozzle. A stationary quasi one-dimensional isentropic compressible fluid flow

a)Author to whom correspondence should be addressed. Electronic mail: francois.sylla@ensta-paristech.fr.
b)Present address: Service des Photons, Atomes et Molcules, Commissariat a l'Energie Atomique, DSM/IRAMIS, CEN Saclay, 91191 Gif sur Yvette, France.

model (1DIFF)[22] gives reliable rule-of-thumbs for millimeter-range nozzles for quickly selecting the nozzle geometry in an ideal situation.

The reduction in size of the jet to the submillimetric range, coupled with the possibility of density variation over several order of magnitude, would give access to laser-Rayleigh-range-long plasmas (even for tightly focussed lasers) from low-density laser transparency to high-density laser opacity regimes. Such an implementation would have tremendous positive impact on systematic investigations of laser-plasma interactions (e.g., parametric instabilites, laser filamentation, relativistic self-focusing, and hole boring). It could also relax the constraints on laser power requirements for users of terawatt-class lasers in studying energetic ion beam generation from gas jets, so far only reported with petawatt-class laser facilities.[7] Importantly and very promising, this type of jet could be a suitable medium for compact and shape-preserving plasma self-compression of ultrashort laser pulse.[23]

However, the broadly used solenoid valve systems which trigger the gas burst then close within typically tens of milliseconds timescale at working pressure ~100 bar "choke" when reducing the throat diameter to sub-millimeter. This property comes from the linear dependence of the mass flow rate in the 1DIFF model with that minimal cross-section in the duct (also called critical diameter). Increasing the pressure to compensate the flow stagnation prohibits subsequent opening of the magnetic-coil-driven poppet, locking increasingly the downstreaming flow. This hinders the exploration of plasma density from microjets in the interval $10^{19} - 10^{21}$ cm^{-3}.

In this paper, we report on the production and the characterization of He gas jet of few hundreds of microns thick with atomic peak densities up to 2.7×10^{21} atoms/cm^3, which corresponds to 1.6 n_c for a singly ionized gas, and drivable at 10 Hz rep rate. This is achieved by using a pressure pneumatic device that allows to boost up the backing pressure up to 400 bar starting from usual gas cylinders (delivering 200 bar at maximum), and a special fast electro-valve with a rise and fall time within 3 ms. This unique association meets the requirements for very dense and thin gas jets compatible with a delicate vacuum pump system.

We smoothly covered experimentally from sonic (Mach number $M \sim 1$) to supersonic ($M > 1$) flow expansions by testing different nozzle geometries from cylindrical to conical ones. With our apparatus, neutral densities $\geq 0.5 n_c$ were only obtained, at exploitable distances from nozzle exit (from few hundreds of microns upwards), with cylindrical of slightly conical nozzles, referring to sonic and transonic flows. This article presents in details only the corresponding experimental results but a sound study of supersonic flows can be found in Ref. 20. Additionally, the real system was characterized with full multiple dimensions computational fluid dynamics simulations in the transient regime. Good agreements with the experimental data are obtained but the simulations underline the sensitivity of the thin flow profile to the precision in the nozzle production. These results will be reported in a future detailed publication elsewhere.

III. SIMPLE ANALYTICAL MODEL: INVISCID FLOW PARAMETERS

This section aims at illustrating qualitatively by using the 1DIFF model, how flow parameters relevant for laser-plasma experiments (density, radial gradient, and mass flow) are expected to vary in steady state according to the nozzle geometry (or equivalently in that model, to the Mach number of the flow, noted M). As mentioned in Ref. 20, one observes an intrinsic competition between the two requirements (i) high peak density during the quasistatic gas expansion in vacuum out of the nozzle and (ii) steep-gradient radial profile with plateau. The position between these two limit cases is essentially quantified by the sonicity, i.e., M. In the following of this document, we will be referring to sonic, transonic, and supersonic flows to describe flows with Mach number, respectively, equal to one ($M = 1$), close to one but larger than one ($M \simeq 1$ and $M > 1$), and equal to several units ($M > 1$). By means of the 1DIFF model, we now explain qualitatively the intrinsic competition between points (i) and (ii) when $M \geq 1$.

(i) The gas density at the nozzle exit is mainly determined by the exhaust gas velocity, i.e., by the conditions of expansion inside the nozzle and thus by the geometry of the nozzle. The 1DIFF model predicts for an ideal gas a simple system of equations linking the cross-sectional area A to the density ρ via the Mach number parameter

$$\frac{\rho}{\rho_0} = \left[\frac{\gamma+1}{2+(\gamma-1)M^2}\right]^{\frac{1}{\gamma-1}}, \tag{1}$$

$$\frac{A}{A_0} = \frac{1}{M}\left[\frac{2+(\gamma-1)M^2}{\gamma+1}\right]^{\frac{\gamma+1}{2(\gamma-1)}}, \tag{2}$$

with A_0 and ρ_0 the cross-sectional area and the density at the throat, respectively, γ is the gas adiabatic constant ($\gamma \sim 1.6$ for helium). It is immediate from (1) that as M increases isentropically the density ρ drops. Considering a sonic flow ($M = 1$), with helium gas at $p = 300$ bar, then $\rho_0 \approx 4n_c$ and $\rho \approx 2n_c$. With the same pressure, for a supersonic flow as in our experiments ($M \simeq 4$), then $\rho \approx 0.2n_c$.

(ii) Ideally, a related Prandtl-Meyer flow can model the expanding fluid that exits the nozzle. This supposes that the pressure in the discharge chamber is way lower than the pressure delivered by the nozzle (underexpanded nozzle), so that the flow adapts via expansion waves. The convex nozzle corners, as defined in Fig. 1 by the angle θ, rotate isentropically the outer layers giving birth to a centered expansion fan through which the fluid is rarefied. The angle of rotation θ_r reads

$$\theta_r = \nu(M_2) - \nu(M_1), \tag{3}$$

$$\nu(M_i) = \sqrt{\frac{\gamma+1}{\gamma-1}}\tan^{-1}\sqrt{\frac{\gamma-1}{\gamma+1}(M_i^2-1)} - \tan^{-1}\sqrt{M_i^2-1}, \tag{4}$$

where $\nu(M_i)$ is the Prandtl-Meyer function, M_1 and M_2 the Mach numbers, respectively, up- and downstream the corner (see Fig. 1 and also for coming implicit symbols). From

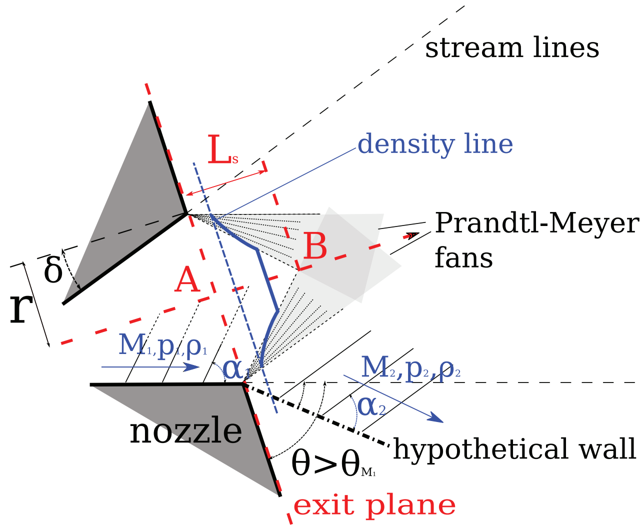

FIG. 1. Isentropic centered Prandtl-Meyer expansion outside a supersonic and underexpanded nozzle (p_{exit} > ambient pressure, p_a). Plateau density radial lines develop over the supersonic length L_s in the inviscid triangle, region between A and B with $M_A \approx M_B$ and delimited by weak density disturbances at Mach angle $\alpha_1 = \sin^{-1}(\frac{1}{M_1})$.

(3) and (4), it follows the existence of a maximum total turn angle θ_{M_1} for a given M_1 above which $M_2 \to \infty$ and p_2 and ρ_2 vanish,

$$\theta_{M_1} = \frac{\pi}{2}\left[\sqrt{\frac{\gamma+1}{\gamma-1}} - 1\right] - \nu(M_1). \tag{5}$$

With helium gas, for a sonic flow, $\nu(M_1) = 0$ and $\theta_{M_1} = 97.3°$. For a supersonic flow as in our experiments ($M_1 \simeq 4$), $\theta_{M_1} = 44.3°$. For all types of flow we produced experimentally, the nozzle corner angle reads $\theta = 70°–90°$. This means that in that model, a sonic flow for which $\theta < \theta_{M_1}$ spreads along the nozzle exit plane, so that the jet will exhibit quite a large radial gradient outside the nozzle. On the contrary, when using a supersonic flow, the convex corner extends over an angle $\theta > \theta_{M_1}$ and the expansion can smoothly develop to ambient pressure (typ. $p_a < 10^{-2}$ mbar). Thus, for the supersonic flow cases, the angular extension of the Prandtl-Meyer fan can be used to assess the radial gradient scale length l at a certain distance Z from the nozzle exit,

$$\frac{l}{Z} \sim \left(\sin^{-1}\frac{1}{M_1} + \theta_{M_1}\right). \tag{6}$$

For $M_1 \simeq 4$, the radial gradients of the jet at $Z = 200$ μm from the exit reads $l \approx 200$ μm. From (6), l/Z reduces, i.e., the jet profile steepens as M_1 increases.

For a supersonic flow, to trade off (i) and (ii) (steep profile along with plateau density), the laser-gas interaction should be operated not too far from the nozzle exit, at a distance $Z \leq L_s$ (see Fig. 1 for the symbol definition),

$$\frac{L_s}{r} = \frac{1}{|\tan(\delta - \alpha_1)|} \tag{7}$$

with r the nozzle exit radius. When cone-sonicity matching is fulfilled, i.e., $\delta = \sin^{-1}(\frac{1}{M_1})$, the ideal supersonic length diverges. In practice, $\delta \neq \alpha_1$ and L_s/r is limited to few units. For $M_1 = 4$, i.e, $\alpha_1 = 14°$ and our supersonic nozzles with $\delta = 20°$ and $r = 200$ μm, one obtains $L_s = 2$ mm.

The mass flow rate $\dot{m}$ for such a system in the 1DIFF model yields

$$\dot{m} = \sqrt{\frac{\gamma}{R}}\frac{p^*}{T^*}\left(\frac{2}{\gamma+1}\right)^{\frac{\gamma+1}{2(\gamma-1)}} A_0 \tag{8}$$

with p^* and T^*, the stagnation pressure and temperature, respectively, (cylinder inlet pressure and room temperature), and R the specific gas constant.

This parameter shows that, for a given nozzle geometry selected according to the Eqs. (1) and (2) to reach a certain sonicity, the mass flow rate and thus the achievable density at the exit is limited by the throat area A_0 (or any smaller area in the flow). Therefore, for designing a jet down-scaled to micrometric dimensions, a proportional increase of the backing pressure must be applied to compensate the rarefaction of the gas. This was done in practice by operating with a backing pressure from ~200 to 400 bar.

IV. EXPERIMENTS

A. Interferometry

The jet characterization was carried out by using a similar setup as the one presented in Ref. 20. In our case, the Mach-Zehnder interferometer stands outside the vacuum chamber and the jet is illuminated by a HeNe 633 nm-CW laser. An *f*/3-doublet images the central plane of the nozzle onto an 8 bit CCD camera. The spatial resolution is about 2 μm and the magnification around 12 (see Fig. 2). Though powerful, this setup has some important limitations which have to be taken into account when characterizing microjets:

- The error (intrinsic noise), assessed by extracting the phase from two consecutive reference images without firing the gas, corresponds to a level of about 10^{18} cm^{-3}. It is mainly due to parasitic vibrations of the interferometer components and therefore requires to shield out the thin beamsplitters from any airstream and to set the assembly on a stabilized optical table.
- The thickness of the microjet is tenfold thinner than usual jets. Therefore the output density has to be at least tenfold higher than in the millimetric case, in order to overshoot the noise level.
- Jets produced by usual millimetric nozzles are often characterized using high refractive index gases such as argon, krypton, …, that give similar profiles as helium, massively used for laser-gas jet interaction, but having a smaller optical index. However, in the present case, when using any of these ersatz at such high pressures, the corruption of the characterization is expected due to the formation of molecular jets with large clusters, as the empirical Hagena parameter $\Gamma^* \geq 10^5$ is much greater than the admitted limit $\Gamma^* \sim 10^3$ for cluster formation.[24–26]

Since the main goal was to produce very dense jets, these points could have been circumvented by using a pneumatic

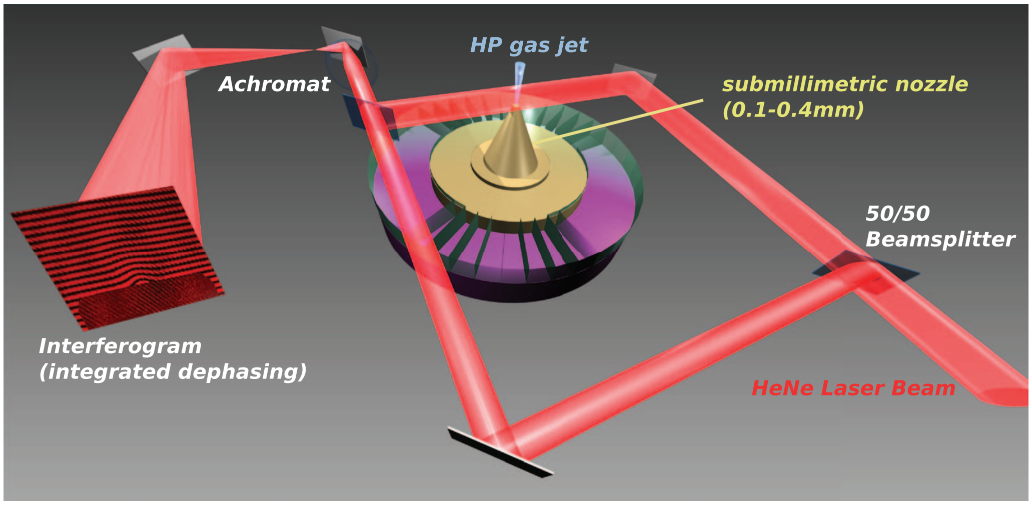

FIG. 2. Mach-Zehnder interferometer with typical interferogram (see Ref. 20) obtained when the high pressure (HP) gas jet is fired.

pressure booster (×75) delivering up to 400 bar of backing pressure.

The phase shift due to the gas is deduced from the interferogram fringe shift with a continuous wavelet transform technique (CWT).[27] A typical raw phase map and the corresponding density calculations at three heights above the nozzle are presented in Figure 3. For the following, we define $n_{ca} = 1.68 \times 10^{21}$ atoms/cm^3 (referred to as atomic critical density). The good axial symmetry of the flow makes the density estimation using the Abel-inversion technique very reliable (estimations with a generalized Abel-inversion assuming non-axisymmetric profiles[28] give the same results).

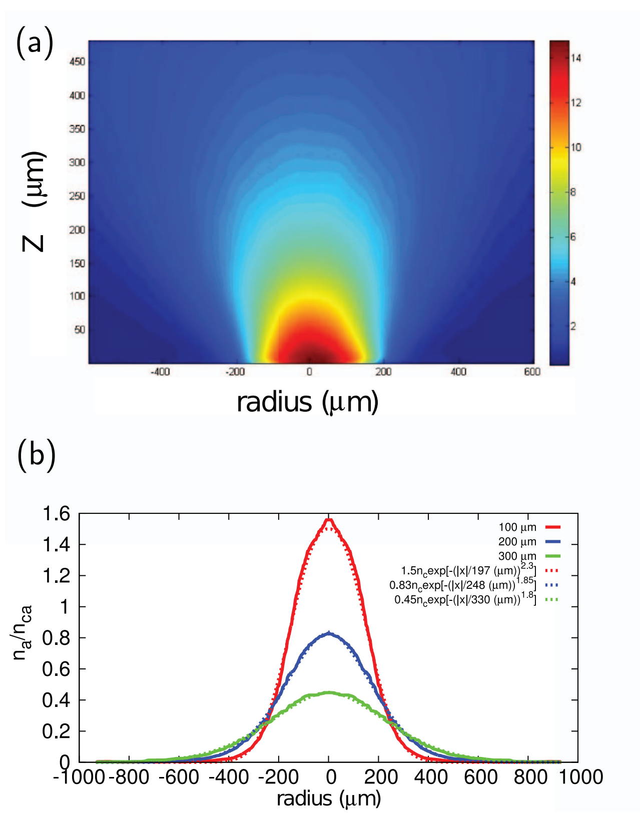

FIG. 3. Data extraction from interferograms obtained with a 400 μm-cylindrical nozzle pressurized at $p = 300$ bar. (a) Phase shift distribution (colormap in radian) from CWT. (b) Neutral He profiles n_a normalized to the atomic critical density n_{ca} at 100 (red line), 200 (blue line), and 300 μm above a 400 μm sonic nozzle from Abel-inversion. The dotted lines indicate the best exponential fits.

B. Innovative apparatus

The He pressure in the upstream reservoir could be in theory varied within the range $p = 50 - 450$ bar. In practice, the pressure was fixed between 300 and 400 bar. This corresponds to mass flow rates of an order of magnitude higher than rates with usual jets used in laser-plasma interaction experiments. However, in this range, the electro-valve we used can fully open and close according to the manufacturer within 3 ms. This fast-switching is made possible by the implementation of the *bid* technology, a recent invention consisting in a bid rotating in an asymmetric induced magnetic field to gate the gas flow out (see Figure 4). This has the advantage to significantly reduce the inertia of the switch and increase the pressure limit by a factor of 10, as compared to translational plastic poppet driven by a spring in usual electro-valve. The conjunction of the fast-switching electro-valve and the high mass flow rate makes the assembly capable of delivering overdense gas jet (see Figure 3), while being usable in the vacuum interaction chamber without endangering the vacuum pump assembly. The stability of the overall system gave a very good shot-to-shot reproducibility in density over the tested pressure range (fluctuations of less than few percent rms).

The method we adopted to vary the density differs from the one usually employed in laser-plasma interaction. Here, the gas pressure feeding the valve is kept constant at $p = 300$ bar because of the long transient regime of the pressure booster, and delays Δt between the gas and the probing laser are varied. Equivalently, Δt can be fixed and the opening time of the valve varied (but this would also result in gas throughput change and hence caution should be practised regarding vacuum pumps). Thus, the interest of this method rests on the fact that the jet profile is determined by

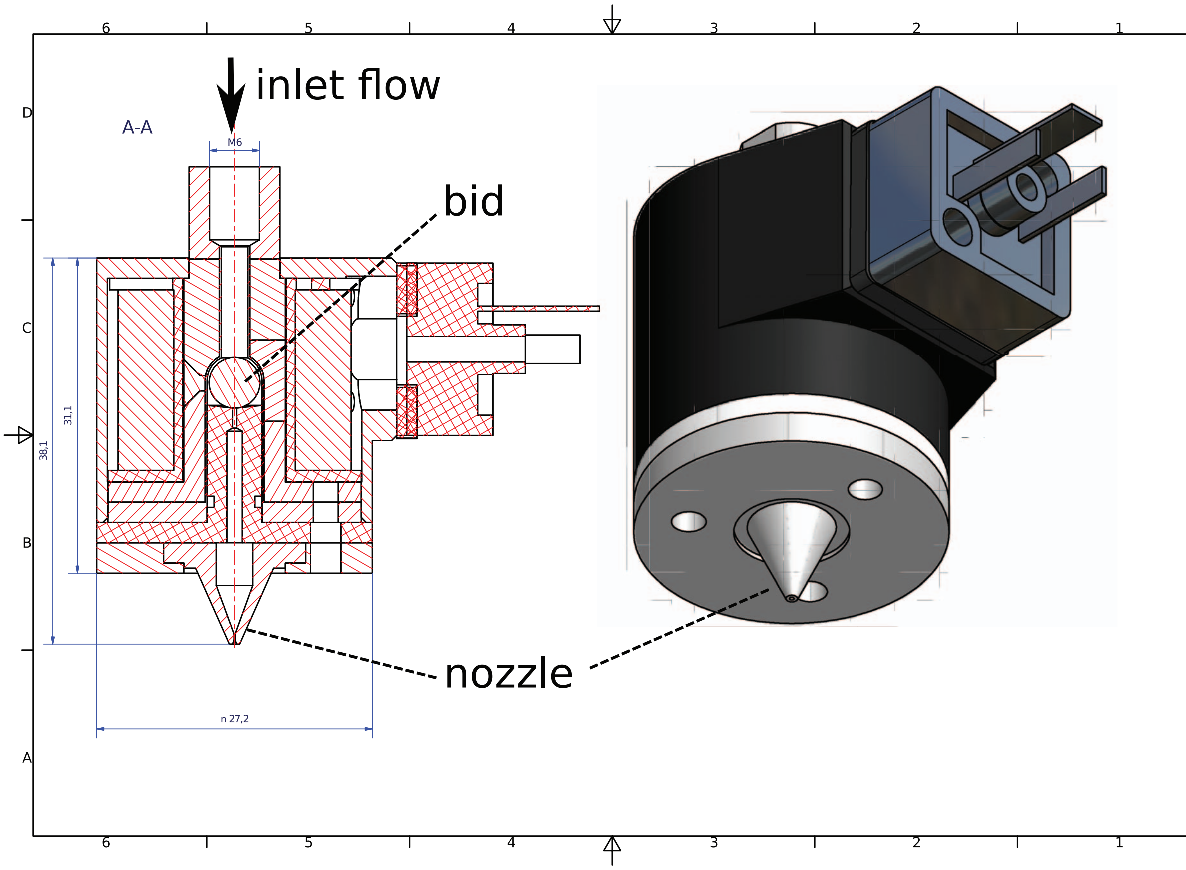

FIG. 4. (Left) Cross-section of the assembly electro-valve + nozzle. The rotating stainless steel bid in the center of the assembly replaces the translational plastic poppet in standard valves. (Right) General outlook of the assembly.

a time, which can be set experimentally much more conveniently than a pressure, and at the precision of the jitter of a simple time-delay pulse generator (with a nanosecond precision).

C. Results

As expected from the 1DIFF model, the spatial profile of the jet depends upon the exit Mach number via the nozzle geometry (ratio of the exit to the critical diameter). This was experimentally verified as shown in Figure 5, where neutral densities normalized to the peak density at 200 μm for each nozzle type are plotted to underline the gradients in radial and vertical directions.

From Eq. (8), the output mass flow rate will be lower in the supersonic case ($A_0 = (100\ \mu\text{m})^2$) than in transonic and sonic ones ($A_0 = (300)^2$ and $(400\ \mu\text{m})^2$, respectively), and so will be the density, for a given stagnation pressure p^*. In our conditions, only the sonic and transonic flows supply neutral densities over 10^{20} cm^{-3}. For the sonic flow the peak density reaches 10^{21} cm^{-3} at 200 μm from the nozzle exit and the flow spreads over 500 μm FWHM. Theses specs make it particularly interesting for an efficient coupling with an ultrashort Ti:Sapphire laser pulse. We describe specifically that high-density flow in the following.

1. *Time dependence*

The time-resolved density at height $Z = 200\ \mu$m is depicted in Figure 6, where the peak densities are plotted against the delay between firing of the valve and the instant of the measurement (instant at which the laser is fired when the interaction is carried out). A typical asymmetric bell shape trendline is obtained and near-critical atomic peak densities are measured at about 20 ms after the valve opening. Despite

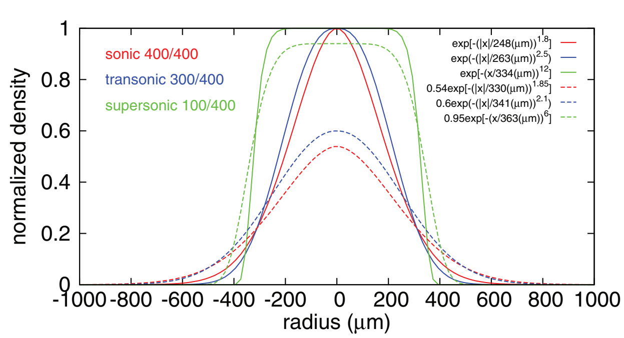

FIG. 5. Sonic (red), transonic (blue), and supersonic (green) flows (best fits) for three nozzles of throat diameters 400, 300, and 100 μm respectively (same exit diameters of 400 μm). The curves are normalized to the peak density at 200 μm. The solid and dashed lines correspond to profiles at 200 and 300 μm from the exit, respectively. Both vertical and radial gradients become larger as the sonicity (Mach number) decreases.

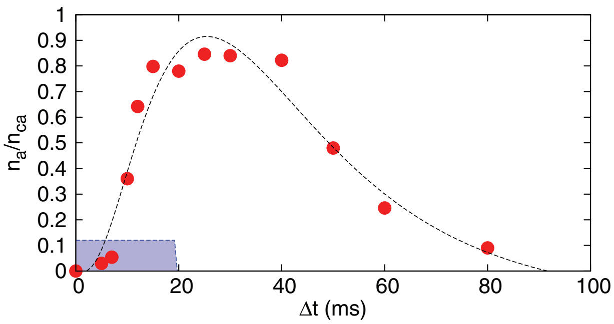

FIG. 6. Time-resolved neutral peak density n_a at 200 μm from the exit of a sonic nozzle (400 μm diameter). The blue region indicates the opening time of the valve. The interpolated dashed line is an indication to guide the reading.

the fast-switching of the valve within 3 ms, the transient state lasts for about 15 ms. This delay is probably due to some kinetic issue in the bid motion that restricts the mass flow rate and causes the "displacement" of the duct smallest area from the nozzle critical diameter down to the valve output orifice, the diameter of which evolving consequently too slowly with time during the opening phase. Optimization of this aspect by changing for instance the bid size and/or the valve housing dimensions will be subject to future developments.

2. *Space dependence*

It is interesting to compare the jet shape at different Δt. Figure 7 presents the jet profiles at $Z = 200\ \mu$m at different delays in the top panel, and the corresponding gradient (ratio of the peak density to the gradient scale length), and gradient scale length in the bottom panel. It appears that the gradient scale length is almost constant over the investigated timespan (red full dots) even if the peak density and thus the gradient vary greatly. Thus, for a sonic nozzle, it is possible to vary the gradient without changing the gradient scale length. This is of utmost importance for carrying out controllable parametric studies on, for instance, laser self-focusing, filamentation instability or electron injection in a density ramp.[29,30]

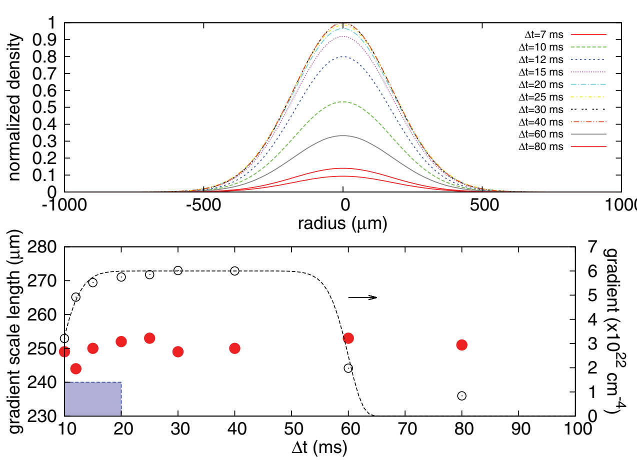

FIG. 7. Profile evolution for different Δt using the same nozzle as in Figure 6. (Top) radial profiles normalized to the peak density at 25 ms. (Bottom) gradient calculated as the peak density over the gradient scale length (black empty dots), and gradient scale lengths from gaussian fits of the profiles (red dots). The blue region indicates the opening time of the valve. The interpolated dashed line is an indication to guide the reading.

V. CONCLUSION

Very dense compact gas jets have been developed for accessing experimentally the critical density limit for Ti:Sapphire laser-plasma interactions at $n_c = 1.68 \times 10^{21}$ cm^{-3}. These new tools enable to safely work in a standard interaction turbo-pumped environment by implementing bid-based electro-valve. The tunability of the jet characteristics (peak density and gradient scale length) from time-delay adjustments opens up opportunities to carry out systematic and exploratory studies of the interaction.

ACKNOWLEDGMENTS

We are pleased to acknowledge the support of the European Research Council for funding the PARIS ERC project (Contract No. 226424), and the ANR-08-NT08-1-38025-1. Finally, the authors acknowledge the support of ANR under the GOSPEL project, grant reference ANR-08-BLAN-0072-03, and the support of OSEO Project No. I0901001W-SAPHIR.

[1] A. Modena, A. Dangor, Z. Najmudin, C. Clayton, K. Marsh, C. Joshi, V. Malka, C. Darrow, D. Neely, and F. Walsh, Nature **377**, 606 (1995).

[2] V. Malka, S. Fritzler, E. Lefebvre, M.-M. Aléonard, F. Burgy, J.-P. Chambaret, J.-F. Chemin, K. Krushelnick, G. Malka, S. P. D. Mangles *et al.*, Science **298**, 1596 (2002).

[3] S. P. D. Mangles, C. D. Murphy, Z. Najmudin, A. G. R. Thomas, J. L. Collier, A. E. Dangor, E. J. Divall, P. S. Foster, J. G. Gallacher, C. J. Hooker *et al.*, Nature **431**, 535 (2004).

[4] C. G. R. Geddes, C. Tóth, J. van Tilborg, E. Esarey, C. B. Schroeder, D. Bruhwiler, C. Nieter, J. Cary, and W. P. Leemans, Nature **431**, 538 (2004).

[5] J. Faure, Y. Glinec, A. Pukhov, S. Kiselev, S. Gordienko, E. Lefebvre, J.-P. Rousseau, F. Burgy, and V. Malka, Nature **431**, 541 (2004).

[6] K. Krushelnick, E. L. Clark, Z. Najmudin, M. Salvati, M. I.K. Santala, M. Tatarakis, A. E. Dangor, V. Malka, D. Neely, R. Allott *et al.*, Phys. Rev. Lett. **83**, 737 (1999).

[7] L. Willingale, S. P. D. Mangles, P. M. Nilson, R. J. Clarke, A. E. Dangor, M. C. Kaluza, S. Karsch, K. L. Lancaster, W. B. Mori, Z. Najmudin *et al.*, Phys. Rev. Lett. **96**, 245002 (2006).

[8] F. Amiranoff, S. D. Baton, S. Huller, V. Malka, A. Modena, P. Mounaix, N. R. Galloudec, C. Rousseaux, and M. Salvati, Phys. Rev. E **61**, 1949 (2000).

[9] V. Malka, J. Faure, S. Hüller, V. T. Tikhonchuk, S. Weber, and F. Amiranoff, Phys. Rev. Lett. **90**, 075002 (2003).

[10] V. Malka, C. Coulaud, J. P. Geindre, V. Lopez, Z. Najmudin, D. Neely, and F. Amiranoff, Rev. Sci. Instrum. **71**, 6 (2000).

[11] S. D. Baton, F. Amiranoff, V. Malka, A. Modena, M. Salvati, C. Coulaud, C. Rousseaux, N. Renard, P. Mounaix, and C. Stenz, Phys. Rev. E **57**, R4895 (1998).

[12] C. Chenais-Popovics, V. Malka, J.-C. Gauthier, S. Gary, O. Peyrusse, M. R.-L. Gloahec, I. Matsushima, C. Bauche-Arnoult, A. Bachelier, and J. Bauche, Phys. Rev. E: Stat. Nonlin. Soft Matter Phys. **65**, 046418 (2002).

[13] J. Denavit and D. W. Phillion, Phys. Plasmas **1**, 1971 (1994).

[14] H. Fiedorowicz, A. Bartnik, Z. Patron, and P. Parys, Appl. Phys. Lett. **62**, 2778 (1993).

[15] E. Fill, S. Borgström, J. Larsson, T. Starczewski, C. Wahlström, and S. Svanberg, Phys. Rev. E **51**, 6016 (1995).

[16] A. Pak, K. A. Marsh, S. F. Martins, W. Lu, W. B. Mori, and C. Joshi, Phys. Rev. Lett. **104**, 025003 (2010).
[17] C. McGuffey, A. G.R. Thomas, W. Schumaker, T. Matsuoka, V. Chvykov, F. J. Dollar, G. Kalintchenko, V. Yanovsky, A. Maksimchuk, K. Krushelnick *et al.*, Phys. Rev. Lett. **104**, 025004 (2010).
[18] J. Faure, J.-R. Marquès, V. Malka, F. Amiranoff, Z. Najmudin, B. Walton, J.-P. Rousseau, S. Ranc, A. Solodov, and P. Mora, Phys. Rev. E **63**, 654 (2001).
[19] V. Malka, J. Faure, J.-R. Marquès, F. Amiranoff, J.-P. Rousseau, S. Ranc, J.-P. Chambaret, Z. Najmudin, B. Walton, P. Mora *et al.*, Phys. Plasmas **8**, 2605 (2001).
[20] S. Semushin and V. Malka, Rev. Sci. Instrum. **72**, 2961 (2001).
[21] V. Malka, J. Phys. IV **133**, (2006).
[22] P. H. Oosthuizen and W. E. Carscallen, *Compressible Fluid Flow* (McGraw-Hill, 1997).
[23] O. Shorokhov, A. Pukhov, and I. Kostyukov, Phys. Rev. Lett. **91**, 265002 (2003).
[24] O. Hagena and W. Obert, J. Chem. Phys. **56**, 1793 (1972).
[25] O. Hagena, Surf. Sci. **106**, 101 (1981).
[26] O. Hagena, Rev. Sci. Instrum. **63**, 2374 (1992).
[27] C. Heil and D. Walnut, SIAM Rev. **31**, 628–666 (1989).
[28] P. Tomassini and A. Giulietti, Opt. Commun. **199**, 143 (2001).
[29] C. G.R. Geddes, K. Nakamura, G. R. Plateau, C. Tóth, E. Cormier-Michel, E. Esarey, C. B. Schroeder, J. R. Cary, and W. P. Leemans, Phys. Rev. Lett. **100**, 215004 (2008).
[30] S. Bulanov, N. Naumova, F. Pegoraro, and J. Sakai, Phys. Rev. E **58**, R5257 (1998).